

Improper monitoring of sewage networks may raise various issues such as overflows, pipe blockages, theft of manhole covers, leading to flooding and pollution, infrastructure damage, vehicles accidents, injury, and even death from falling into open manholes. The key objective of this research was to examine different elements and create a prototype architecture for a real-time sewer monitoring system. Implementation of the architecture involved constructing a data gathering station and experimenting with various wireless sensing devices to assess the precision of the sensors. In addition, the study sought to design a geographic information system that integrates algorithms capable of identifying sewer overflow, blocked pipes, and the presence of manhole covers. The performance of Sharp GP2Y0A41SK0F infrared, TF-Luna Benewake LiDar, TOF400 VL53L1X laser, JSN-SR04T ultrasonic distance sensors was tested in terms of their ability to monitor water level and manhole cover. Tests revealed the most favorable results in TOF400 VL53L1X at distances between 0.2 and 1.0 m (presumed distance to the manhole cover) with a standard deviation of 0.13–0.24, and in TF-Luna Benewake at distances between 1.0 and 5.0 m (presumed distance to the chamber bottom) with a standard deviation of 0.44–1.15. The deviation analysis has yielded equations that can be utilized to provide rough estimates of the accuracy levels of the aforementioned sensors, based on the measured distance. Additionally, the FC-28 analog and YL-63 infrared sensors were evaluated for detecting pipe blockages, with the YL-63 being more suitable. The outcomes of this study furnish valuable insights that can aid in achieving sustainable resolutions for issues related to sewer monitoring

Keywords: *sewer monitoring, sensors, Internet of Things, Geographic Information System, sewer chamber*

PROTOTYPING AN INTEGRATED IOT-BASED REAL-TIME SEWER MONITORING SYSTEM USING LOW-POWER SENSORS

Yelbek Utepov

PhD, Professor

Supervisor of Research Projects*

Professor**

Alexandr Neftissov

PhD, Associate Professor, Director

Research and Innovation Center «Industry 4.0»***

Timoth Mkilima

PhD, Senior Researcher*

Assel Mukhamejanova**

PhD, Senior Lecturer*

Department of Civil Engineering

Shyngys Zharassov**

MSc, Junior Researcher, PhD Student*

Alizhan Kazkeyev**

MSc, Junior Researcher, PhD Student*

Andrii Biloshchytskyi

Corresponding author

Doctor of Technical Sciences, Professor, Vice-Rector of the Science and Innovation***

Department of Information Technology

Kyiv National University of Construction and Architecture

Povitroflotskyi ave., 31, Kyiv, Ukraine, 03037

E-mail: bao1978@gmail.com

*Solid Research Group (LLP)

B. Momyshuly str., 17A, Astana, Republic of Kazakhstan, 010010

**Department of Civil Engineering

L. N. Gumilyov Eurasian National University

Satpayev str., 2, Astana, Republic of Kazakhstan, 010008

***Astana IT University

Mangilik Yel ave., 55/11, C1, Astana, Republic of Kazakhstan, 010017

Received date 09.04.2023

Accepted date 16.06.2023

Published date 30.06.2023

How to Cite: Utepov, Y., Neftissov, A., Mkilima, T., Mukhamejanova, A., Zharassov, S., Kazkeyev, A., Biloshchytskyi, A. (2023).

Prototyping an integrated IoT-based real-time sewer monitoring system using low-power sensors. *Eastern-European Journal of Enterprise Technologies*, 3 (5 (123)), 6–23. doi: <https://doi.org/10.15587/1729-4061.2023.283393>

1. Introduction

The sewer system is an essential component of modern urban infrastructure that handles wastewater and other forms of liquid waste [1]. However, sewer systems are prone to various problems such as blockages, overflows, leaks, and the presence of open manhole covers. The consequences of such problems can be severe and wide-ranging. Blockages,

overflows, and leaks can lead to the contamination of the environment, including water sources and soil, posing a risk to human and animal health. Sewage overflows can also cause property damage and unpleasant odors and can attract insects and rodents. A healthy city's ecosystem also depends on the waste management system [2, 3]. Due to a lack of understanding, people frequently throw trash onto highways, allowing soluble trash like polythene and plastic bottles

to enter sewer lines and clog drainage systems. Manually locating the congested spot is really challenging. Maintenance entails a significant time commitment, financial loss, and severe human suffering. Open manhole covers pose a significant risk to public safety as they can cause accidents and injuries to pedestrians, cyclists, and motorists. They can also act as an entry point for pollutants, debris, and hazardous materials into the sewer system, exacerbating existing problems [4, 5]. To prevent these problems, it is essential to monitor the sewer system's condition and take preventive measures before a catastrophic event occurs [6].

Traditionally, sewer systems are monitored through physical inspections of sewer pipes, manholes, and their covers [7]. This involves sending workers down into the sewer system to inspect the pipes manually by performing a range of activities, such as visual inspection [8], smoke testing [9], dye testing [10], acoustic monitoring [11], Closed-circuit television (CCTV) inspection [12], Ground-penetrating radar (GPR) [13], flow measuring [14], etc. However, these methods are hazardous and time-consuming and have several limitations, such as safety risks, inaccuracies, limited coverage, reactive maintenance, limited data, weather dependency, and limited access [15]. In this context, the development of sewer monitoring systems using modern technologies has become increasingly important, as they provide real-time data on the sewer system's performance even without human intervention [16]. For example, Internet of Things (IoT) technology has emerged as a very practical strategy in the modern world, which is more data-driven and automated. The IoT system is made up of internet-connected devices that can wirelessly exchange data without human intervention. Currently, the IoT connects vehicles, refrigerators, lighting, and all other kinds of gadgets. In a nutshell, the IoT gives a chance to construct and manage a system effectively and affordably [17]. The monitoring of sewer systems heavily relies on sensors. The selection of an appropriate sensor is a critical aspect of the sewer monitoring system's design, as it affects the accuracy and reliability of the data collected. The use of sensors that are not suitable for the monitoring task can lead to inaccurate data, which can result in ineffective decision-making and costly remediation efforts [18–20].

Therefore, research devoted to the prototyping of an integrated IoT-based real-time sewer monitoring system using low-power sensors is relevant.

2. Literature review and problem statement

A review of recent studies in the field of sewer system monitoring revealed the presence of diverse solutions to monitor sewer systems incorporating sensors and IoT concept. Thus, [21, 22] proposed an IoT-based sewer monitoring system capable of tracking the dynamic change in humidity, temperature and gas concentration. The study incorporated methane (MQ-4), carbon dioxide (MQ-7), humidity and temperature (DHT11) sensors along with Raspberry Pi 3 (Model B) single-board computers, GSM module and ThingSpeak IoT communication software. The integration of a camera is also considered. The system sends alerts in case of exceeding the threshold of the aforementioned factors. Similarly, [23] offered a working model for a smart manhole monitoring system using the same components. Despite the simplicity of these solutions, they have unresolved issues in system architecture related to the use of disparate components, which often cause interopera-

bility problems and are inflexible. In addition, the limited capabilities of ThingSpeak may be inadequate to handle the enormous flow of data from an entire city sewer system. The authors of the study [24] argues that a ZigBee technology can solve interoperability issues between products from various manufacturers. The study incorporates the ZigBee module operating on IEEE 802.15.4 standard to remotely control sensors. However, ZigBee has a short range of 10–100 m and a low rate of data transfer of up to 250 kbit/s, which is rather weak for the purpose of monitoring sewer systems. Moreover, it is not free and costs considerably. Unlike previous studies, [25] presented a review of IoT solutions to control various parameters of water storage tanks. The review provides insights into the wide range of microelectronic components used for water tanks but not limited to be used for other purposes. Some of the components that are of interest for current research include electronic development kits (Arduino, Raspberry Pi, NodeMCU) and sensors (ultrasonic, LiDAR, laser, analog). A review by [26] examines acoustic and ultrasonic technologies for inspecting water and sewerage pipes. It discusses accelerometers, hydrophones, fiber-optic sensors, bulk wave, and guided wave sensors, which have gained interest due to their sensitivity, flexibility, speed, and adaptability to complex situations. The above reviews consider a fairly large variety of sensors solutions and their applications. However, they miss an important solution to the issue of monitoring manhole cover presence. The study by [27] proposes a sewage blockage detection system based on IoT. The system is capable of sending and visualizing alerts when the threshold values are crossed. Its primary components are: multiple sensing devices, centralized gateway and web-based dashboard with an interactive map. The prototype of the sensing device was built using HC-SR04 ultrasonic sensor, MQ4 methane gas sensor, MPU6050 inertial measurement unit, and GSM SIM800A run by Raspberry Pi. A personal computer (PC) is arranged as a gateway between the Raspberry Pi and the dashboard. With appropriate development, this system has the potential to succeed. However, it is worth noting that using GSM as a communication standard makes the solution expensive and dependent on network providers. Moreover, the usage of a PC as a gateway limits transportability. With a similar approach earlier [28] proposed a web GIS solution for monitoring urban sewage pipelines that plots sensory data on an interactive map by means of various web map services. The approach is noteworthy, but insufficiently elaborated, and only pipeline monitoring is considered using ultrasonic sensors. In addition, the solution proposed does not provide any details about interfaces connecting sensors and GIS, i.e. there is no clarification on how the data is transferred from sensors to GIS. The author only mentions some middleware, but gives no information on which type of middleware.

Literature review [21–28] showed that the existing solutions for sewer monitoring are way far from being applied in actual practice. Thus, the following problems can be stated:

- the solutions considered have poor system architecture, which may result in material and labor costs;
- the majority of solutions are at the conceptual stage, with no specially designed PCB and case, as well as their performance is not tested and evaluated;
- the considered solutions have neither complete GIS for real-time monitoring of sewer overflow, blocked pipes, and manhole covers presence, nor their algorithms.

All of this suggests the necessity to conduct research on the prototype development of an integrated IoT-based real-time sewer monitoring system using low-power sensors.

3. The aim and objectives of the study

The study aims to develop a prototype of an integrated IoT-based real-time sewer monitoring system using low-power sensors. This will make it possible to achieve long-lasting, affordable and reliable sewer monitoring by utilizing low-power microelectronic components and wireless technologies, ensuring continuous operation even in challenging environmental conditions. Furthermore, the integration of web-based GIS technology will allow an interactive and user-friendly representation of monitoring data, enabling efficient analysis and informed decision-making, as well as allowing for a comprehensive assessment of an entire city’s sewer system.

To achieve the aim, the following objectives are accomplished:

- to design a prototype architecture for a real-time sewer monitoring system (RTSMS) by exploring different elements;
- to build a data gathering station (DGS) and wireless sensing devices (WSD), and estimate the cost of materials;
- to test and evaluate the accuracy of various integrated sensors;
- to design algorithms capable of detecting sewer overflow, blocked pipes, and presence of manhole covers using integrated sensors;
- to develop a web-based Geographic Information System (GIS).

4. Materials and methods

The object of current research is a prototype of an integrated IoT-based real-time sewer monitoring system using low-power sensors. The main hypothesis of the study is that by utilizing low-power microelectronic components, IoT and GIS technologies, it is possible to achieve low-cost and long-lasting sewer monitoring, which enables interactive and real-time assessment of an entire city’s sewer system. The research assumes that the LiDAR, laser and infrared sensors along with wireless communication technologies are suitable for sewer monitoring purposes. It assumes that

the sensors’ performance and accuracy can be evaluated based on their ability to monitor water levels, manhole covers, and sewer pipes. Furthermore, it assumes that the integration of algorithms and GIS technology will provide effective means of detecting sewer overflow, blocked pipes, and manhole cover presence or absence. The research simplifies the sewer monitoring system by focusing on a prototype architecture and using low-power sensors. It also simplifies the analysis by employing distance measurements and Boolean outputs from the sensors to determine the status of various parameters such as wastewater levels, manhole cover presence, and pipe blockages. The cost estimation is based on the prototype implementation and may not account for all possible variables in a real-world scenario.

The RTSMS prototype was developed using the sequential and linear approach known as the “waterfall model”, which involves gathering requirements, designing the system architecture, implementing it, and verifying its functionality, as proposed by [29].

The prototype was given the following primary requirements:

- wireless sensing: the system should comprise a wireless multisensory device that can detect various parameters such as sewer overflow, pipe blockages, and manhole cover opening/closing;
- data gathering: the system should comprise a data gathering station to collect data from wireless sensing devices;
- GIS integration: the system should integrate with GIS technology to display collected data on an interactive map;
- real-time monitoring: the system should be capable of early warning and predicting sewer problems;
- user-friendly interface: the system should have a user-friendly interface that is easy to understand and use for various user roles;
- cost-effectiveness: therefore, the system must be cost-effective in the long run.

To design the system architecture, the study considered a variety of electronic components, from which different combinations of the system were assembled and tested. Their specifications are presented in Tables 1–5 below.

Table 1

Specification of sensors

Characteristics	Sharp GP2Y0A41SK0F [30]	TOF400 VL53L1X [31]	JSN-SR04T [32]	TF-Luna Benewake [33]	FC-28 [34]	YL-63 with LM393 comparator [35]
Sensor type	Infrared	Laser	Ultrasonic	LiDAR	Analog	Infrared
Voltage, V	4.5–5	3–5	5	5	3.3–5	3.3–5
Amperage, mA	30	40	30	70	15	120
Interface type	analog	digital	digital	digital	analog, digital	analog, digital
Connection pins	V0, GND, VCC	VIN, GND, SCL, SDA, XSHUT, GPIO1	VCC, GND, TRIG, ECHO	VCC, GND, RX, TX	VCC, GND, D0, A0	VCC, GND, OUT
Measurement range, m	Up to 0.3	Up to 4	Up to 5	Up to 8	–	Up to 0.3
Operating temperature, °C	–10 to 60	–20 to 70	–10 to 70	–20 to 75	–40 to 60	–20 to 80
Dimensions, mm	29.5×13.0×13.5	17×18×7	41×28.5	30×21.25×13.5	20×60	43×16×7
Price*, USD	9.68	18.15	14.04	24.90	1.23	0.65

Note: * – since the components were purchased locally, the prices were converted according to the exchange rate for the date 31.03.2023 [36], which was 448.05 KZT for 1 USD

When choosing sensors, several parameters were taken into account. The availability on the market, cost, power consumption level, operating principle, debugging complexity, and the availability and type of data interfaces were considered for comparison. All sensors have different power consumption levels and technical parameters, including the measurement principle. It is not possible to immediately determine the suitability of a specific sensor based on its technical characteristics. It was important for us to conduct experimental research and determine the possibility of using each of the sensors in combination with others. The plan was to evaluate several distance measurement sensors, including the Sharp GP2Y0A41SK0F, TOF400 VL53L1X, JSN-SR04T, and TF-Luna Benewake, to detect the presence of a manhole cover and potential overflow. It was assumed that sensors would measure the distance between the manhole cover and the liquid surface at specific intervals. If there was a sharp deviation from the previous values, either one or both cases would arise.

For identifying pipe blockages, two sensors, the FC-28 and YL-63, were chosen as they may offer the necessary functionality. The idea for the pipe blockage sensor was to identify the critical level of silt or debris based on electrical conductivity (in the case of FC-28) or optical (for YL-63) observation. However, while investigating the FC-28, we identified its unsuitability. This sensor correlates the electric conductivity with the moisture content in the silt and in case of debris, it may produce biased records. Besides, it is likely that both in the absence and presence of pipe blockages, the moisture would be almost constant, except for those rare instances when the liquid is not flowing in pipes. In addition, the brittle parts of FC-28 are not protected against external loads (e. g., liquid flow), and may be broken immediately.

Table 2

Specification of microcontrollers

Characteristics	ATmega328P [37]	ESP8266MOD [38]
Manufacturer	Microchip Technology/Atmel	Espressif Systems
Processor core type	AVR	Tensilica L106
Program memory size, kB	32	50
Maximum clock frequency, MHz	20	160
Data bus width, bit	8	32
Operating voltage, V	2.7 to 5.5	2.5 to 3.6
Amperage, mA	0.01 to 0.8	80
Interface type	I2C, SPI, USART	I2C, SPI, USART, SDIO, I2S, IR
ADC	8×10b	1 channel
IEEE 802.11 support	–	b/g/n/d/e/i/k/r
Operating temperature, °C	–40 to 125	–40 to 125
Dimensions, mm	7×7×1	24×16×4
Printed circuit board (PCB)	Custom printed	NodeMCU [39]
Price*, USD	6.2	6.74**

Note: * – since the components were purchased locally, the prices were converted according to the exchange rate for the date 31.03.2023 [36], which was 448.05 KZT for 1 USD; ** – total price for NodeMCU firmware including ESP8266MOD microcontroller

The ATmega328P microcontroller was used to assemble a WSD. It has the necessary technical characteristics that

allowed the required functions to be performed: collecting data from sensors, processing them, and transmitting them using the Serial Peripheral Interface (SPI). The main advantage is its low power consumption, which is important for autonomy. The presence of additional interfaces allowed for the use of wireless modules for data transmission. This also allowed for the necessary level of autonomy. The clock frequency and memory capacity are sufficient to implement the functionality.

The ESP8266MOD microcontroller was used to assemble a DGS. It is commonly incorporated into the NodeMCU firmware [39]. The feature of choosing it is the ability to connect wirelessly via Wi-Fi. The SPI interface also allows for the connection of other wireless or other modules simultaneously. Hence, we connected a RobotDyn SD card module [40] and utilized a microSD card (together cost 4.5 USD) to temporarily store the sensing data in case of Wi-Fi failure. Since autonomy was not a concern for the DGS, an important criterion was the ability to connect multiple types of wireless communication, sufficient memory capacity for the program and storing collected data from the moment of reception until successfully transmitted to the server.

The microcontrollers used have open-source code, which allows for easy configuration to suit specific needs, maximizing adaptability and optimization.

Table 3

Specification of communication modules

Characteristics	Lora Ra-02 on the SX1278 chip [41]	Wi-Fi within ESP8266 ESP-12F [38]	SIM800L GSM/GPRS [42]
Manufacturer	Ai-Thinker	Espressif Systems	SIMCom
Communication protocol	LoRaWAN	Wi-Fi	GPRS
Operating voltage, V	2.5 to 3.7	2.5 to 3.6	3.4 to 4.4
Amperage, mA	12.15	80	2,000
Frequency range, MHz	433	2,400 to 2483.5	850 to 1,900
Communication distance, m	Up to 10,000	Up to 50	Within the coverage area
Transmitting power, Mbps	Up to 0.027	Up to 54	Up to 0.856
Operating temperature, °C	–30 to 85	40 to 125	–40 to 85
Dimensions, mm	17×16×3.2	24×16×4	15.8×17.8×2.4
Price*, USD	7.63	Counted in NodeMCU	8.88

Note: * – since the components were purchased locally, the prices were converted according to the exchange rate for the date 31.03.2023 [36], which was 448.05 KZT for 1 USD

The proposed system involves the use of IoT, which is why various data transmission interfaces were used. When building the system and selecting the types of communication, the volume of traffic, power consumption, and the ability to use the system without obtaining permission from network providers and government agencies were taken into account.

Low power consumption and long-distance communication are important criteria for transmitting data from WSD due to the extensive area coverage. Therefore, the choice was made to use LoRaWAN. This type of communication allows data to be transmitted up to 100 m, with an operating current of only

12.15 mA and an even lower current in standby mode. Power consumption during operation is very low, which significantly increases the battery life. The bandwidth for the planned data is more than sufficient.

For receiving data at DGS, LoRaWAN was also used, and for further transmission to the server, Wi-Fi was used. This is because DGS will have a constant external power source and there are no restrictions on power consumption, and it will be installed within the coverage range. The use of GPRS was also considered, but the SIM800L module requires a power source with an output voltage of 3.4 to 4.4 V and a maximum operating current of 2 A, which would complicate the design and reduce reliability. Therefore, it was decided to transmit data to the server using Wi-Fi.

Table 4

Specification of cases

Characteristics	RYD-F3-2 [43]	Custom, as in [44]
Manufacturer	Digital Zakka	Handmade
Material	Acrylonitrile butadiene styrene (ABS)	Two-component polyurethane
Waterproof	IP67	IP67
Dimensions, mm	115×90×55	200×85×65
Price*, USD	10	1.2

Note: * – since the components were purchased locally, the prices were converted according to the exchange rate for the date 31.03.2023 [36], which was 448.05 KZT for 1 USD

Table 5

Specification of power suppliers

Characteristics	LS 14500 [45]	RS-15-5 [46]
Manufacturer	SAFT	Mean Well
Type of power supply	Battery	Transformer
Type of current	DC	AC/DC
Output power, W	–	15
Output voltage, V	3.6	5
Output current, A	–	3
Nominal capacity, Ah	2.6	–
Nominal energy, Wh	9.36	–
Input voltage range, V	–	85 to 264
Operating temperature, °C	–60 to 85	–20 to 70
Battery holder	Included	–
Dimensions, mm	Ø14.62×50.28 (AA)	62.5×51×28
Price*, USD	6	9.67

Note: * – since the components were purchased locally, the prices were converted according to the exchange rate for the date 31.03.2023 [36], which was 448.05 KZT for 1 USD

The plastic case RYD-F3-2 made of ABS was chosen for the WSD. This case is waterproof to IP67 standard and can suit in size and shape electronic components, as well as reliably protect them from liquid and dust particles. It also has four holes on the edges that are optimal for fastening to an anchor. The DGS case was handmade using a two-component liquid polyurethane molding and casting method. It took no more than one minute from casting to achieve sufficient strength. Both cases consisted of two plastic parts – a container and a lid. The lids were fastened to the containers with four screws. Rubber gaskets were provided in both cases to seal the lid's perimeter groove. To prevent fogging and condensation, silica gel packets were intended to be placed inside the cases together with electronic components.

The LS 14500 batteries were chosen to power the WSD. These batteries are distinguished by their high frost resistance and long service life. For powering the DGS, the RS-15-5 switching power supply transformer was selected to convert high voltage current to a level acceptable for the ESP8266MOD microcontroller. The selected power sources have compact dimensions, making them easy to fit inside the cases.

Along with electronic components, various IT solutions were utilized during the development of RTSMS. Thus, Eagle [47] (56 USD per month) software was used to design the PCBs for WSD and DGS in Gerber format. An Arduino IDE [48] open-source cross-platform software was used to program the PCBs. A MariaDB [49] open-source relational database was used to store the data received from DGS. A Spring Boot [50] open-source framework was used to run the back end. An open-source React JS [51] and OpenLayers APIs [52] were used to develop a front end (i. e., an interface of a GIS).

The manufacturing of PCBs was carried out at Astana IT University (Astana, Kazakhstan). The NodeMCU based on ESP8266MOD was soldered to the DGS PCB along with SX1278, SD card module, and DS3231 real-time clock (RTC) [53] (4 USD). The RS-15-5 was connected to DGS PCB using copper wires. A line cable with Schuko plug 230 V (2 USD) was attached to RS-15-5 using its screws. All the electronic components were placed inside the handmade DGS case.

The ATmega328P, SX1278, and AA battery holder were soldered to the WSD PCB along with other necessary microcomponents and were placed into the RYD-F3-2 case. The sensors were connected using copper wires. A total of three WSD combinations were initially assembled and programmed with Arduino IDE, differing only in the sensors for monitoring the wastewater level and manhole cover:

- 1) Sharp GP2Y0A41SK0F for measuring the wastewater level, and JSN-SR04T for detecting the manhole cover presence.
- 2) TF-Luna Benewake for both measuring the wastewater level and detecting the manhole cover presence.
- 3) TOF400 VL53L1X for both measuring the wastewater level and detecting the manhole cover presence.

A test setup was prepared to evaluate the suitability of each sensor for its intended functionality (Fig. 1) that horizontally imitates a sewage well.

As shown in Fig. 1, WSD was installed on the floor dividing it into two parts. The obstacles placed on the left and right parts of the floor were used to imitate the wastewater level and the manhole cover cap bottom. It was assumed that the WSD would be installed inside a standard manhole at a depth not exceeding 1 m. Therefore, we marked test distances on the right part of the floor at intervals of 20 cm up to 1 m. For the left part, test distances were marked on the floor at intervals of 1 meter up to 5 meters. For each marked distance, each sensor (right and left) had to make 100 measurements with an interval of 5 seconds. The same procedure is repeated for each WSD combination. For this stage, the DGS prototype was connected to a laptop directly through USB and collected measurement data from WSD via LoRaWAN. The gathered data was visualized on charts to assess the performance of the sensors and streamline the selection process. Additionally, to evaluate the accuracy of the sensors, we calculated the average deviations from the intended distances and illustrated them on a graph. This helped to make the final choice of sensors for monitoring the manhole cover and wastewater level.

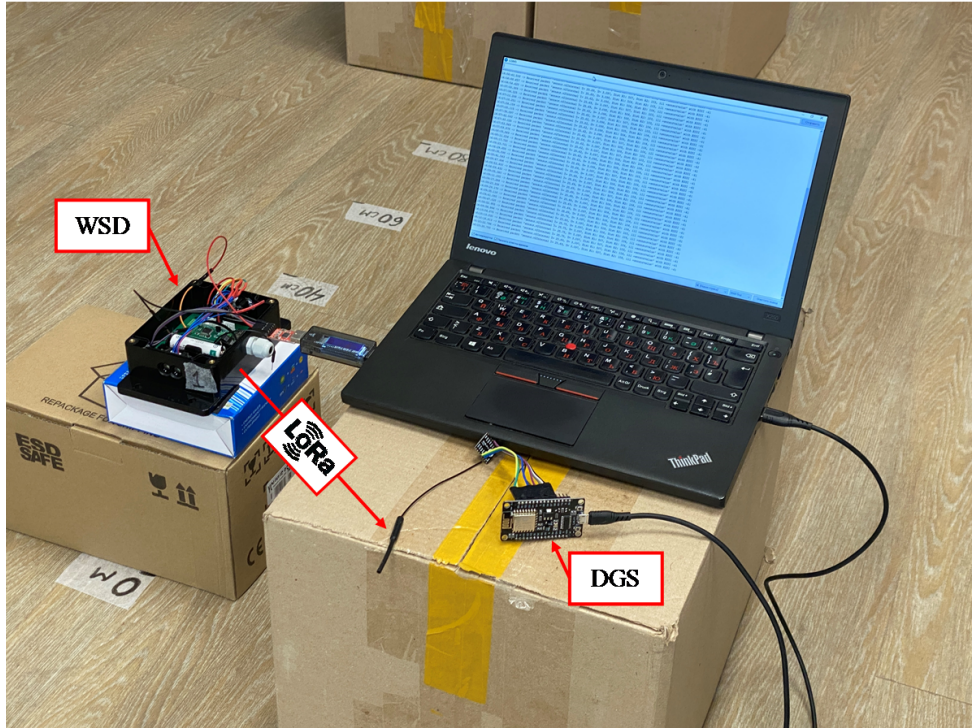
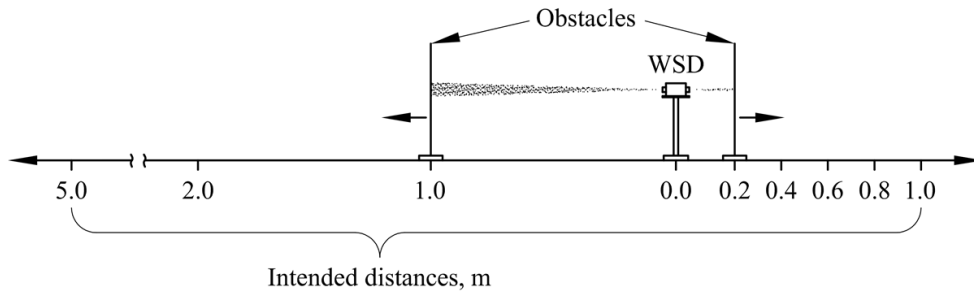


Fig. 1. Test setup

To monitor pipe blockages, an infrared sensor YL-63 was incorporated into the WSD as an externally assembled module. The module consists of two parts, where an infrared emitter and a photoreceiver of the YL-63 sensor are positioned against each other. The cases of both module parts are made of transparent plastic to allow the thermal radiation to pass through freely. Unlike the aforementioned sensors, the YL-63 did not require information about the distance to the presumed object, only its presence or absence. Thus, the operating principle of the external module was as follows. Radiation is reflected from the obstructing object (wastewater or silt) and is detected by the photoreceiver, which then sends a signal to the LM393 comparator, which is set to trigger at a certain level of photoreceiver illumination. The LM393 comparator generates a low or high-logic-level signal at the sensor output. The module operates by detecting the level of illumination of the photoreceptor. Since the sensor detects reflected radiation, there may be an error in measuring the distance due to the varying reflective properties of obstructing surfaces made of various materials. Therefore, the pipe blockage module was calibrated to detect materials such as wastewater and silt based on their reflective properties.

5. Results of the prototype development of an integrated IoT-based real-time sewer monitoring system using low-power sensors

5.1. Prototype architecture for a real-time sewer monitoring system

After considering various electronic components and software solutions, the most suitable IoT architecture for the RTSMS was formed and is presented in Fig. 2 below.

As shown in the system architecture above, the RTSMS is composed of WSDs installed in sewer wells that send measurement data through LoRaWAN to the DGS located nearby. The DGS collects the data and sends it through Wi-Fi and an Internet modem to the server side. The server side is built with a MariaDB open-source relational database and is powered by a Spring Boot open-source framework with REST API business logic on the back end. Currently, it is hosted in the Astana IT University. The front end of the system is developed using React JS and OpenLayers APIs, along with HTML, JavaScript, and CSS codes, to provide a user-friendly and interactive interface to visualize the data through a web browser on the client side. It makes HTTP requests to the back end to retrieve the collected data in a JSON format.

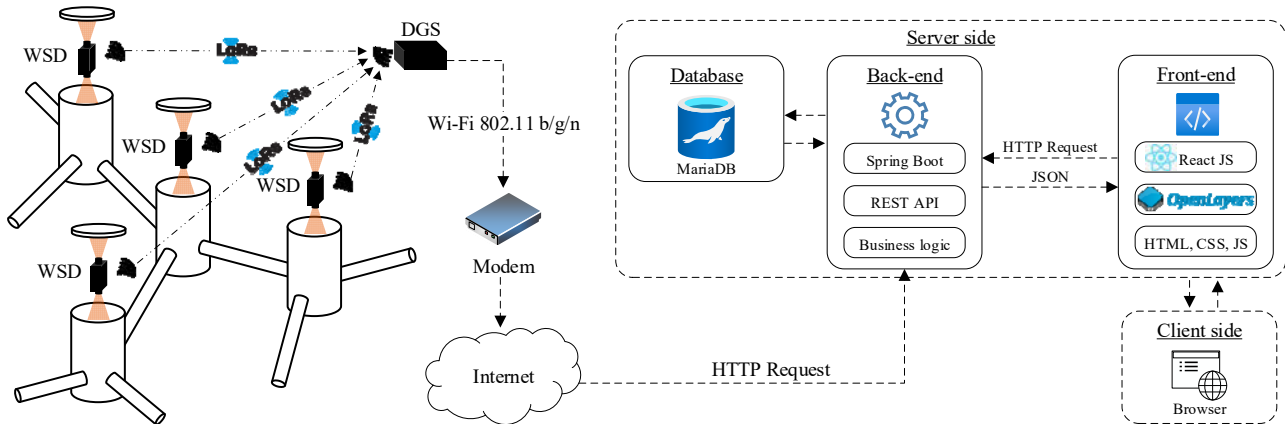


Fig. 2. RTSMS system architecture

5. 2. Data gathering station and wireless sensing devices

Fig. 3 below shows a circuit diagram and a PCB design of the DGS.

As shown in the circuit diagram above, the DGS was assembled by connecting the LoRa Ra-02, DS3231 RTC, and RobotDyn SD card modules to the NodeMCU firmware by means of a 77×87 mm PCB that was designed using Eagle and manufactured at Astana IT University. Before assembling, it was important to identify the pins on each module and determine the appropriate connection interfaces. We used 11 input-output pins of NodeMCU to connect the modules. Thus, the D0, D3, D4, D5, D6, D7, 3V3, and GND pins of NodeMCU were connected to the RESET, NSS, DIO0, SCK, MISO, MOSI, 3.3V, and GND pins of the LoRa Ra-02 module, respectively. The D1, D2, 3V3, and GND pins of NodeMCU were connected to the SCL, SDA, VCC, and GND pins of the DS3231 RTC module, respectively. While the D5, D6, D7, D8, 3V3, and GND pins of NodeMCU were connected to the D5, D6, D7, D8, 3V3, and G pins of the RobotDyn SD card module, respectively.

Fig. 4 below shows a circuit diagram and a PCB design of the WSD.

As shown in Fig. 4 above, the circuit diagram was presented for the WSD combination No. 1, where the Sharp GP2Y0A41SK0F and JSN-SR04T sensors were utilized for measuring the wastewater level and detecting the manhole cover presence, respectively. The electrical circuits of the other combinations are analogous. The WSD was built using an ATmega328P chip that contains firmware for processing sensor data and transmitting it using the 433 MHz LoRa Ra-02 communication module. Power is provided by three AA batteries of the LS 14500 brand. The LoRa module is connected using pins D7, D9, D10, MISO, MOSI, and SCK. The PCB has three interfaces for sensor connection, two of which are I2C, and one for connecting a discrete sensor. The third connector allows for the connection of a sensor via a serial interface. The JSN-SR04T sensor is connected via the serial interface. The Sharp GP2Y0A41SK0F sensor is connected using pin A2 for the analog sensor connection. The YL-63 sensor is connected to pin D3. The PCB has a power switch.

Fig. 5 shows the assembled view of the WSD prototype in various combinations of sensors for monitoring overflows and manhole cover, along with the pipe blockage monitoring module, as well as the typical schema to install the WSD.

As shown in Fig. 5 above, all the inner electronic components of WSD fit into the RYD-F3-2 case. The walls of the case were drilled depending on the type of sensor used, and the YL-63 module was assembled externally. The latter was made of two identical transparent plastic capsules connected on a single metal plate, one storing the YL-63 LM393 comparator and photoreceiver, and another storing the emitter. The bottles have been tightly sealed to ensure a hermetic closure, while also being secured in place to keep the photoreceiver and emitter in close proximity to each other, with a distance of only 3–5 mm between them. According to the provided schema, the WSD should be fixed on the sewer well at a recommended depth of under 1 m. The YL-63 module should be connected to WSD using sealed wires. It should be mounted on the wall of the discharge pipe at a midpoint height so that it can detect a critical instance of blockage when the silt level reaches the halfway point of the discharge pipe’s radius.

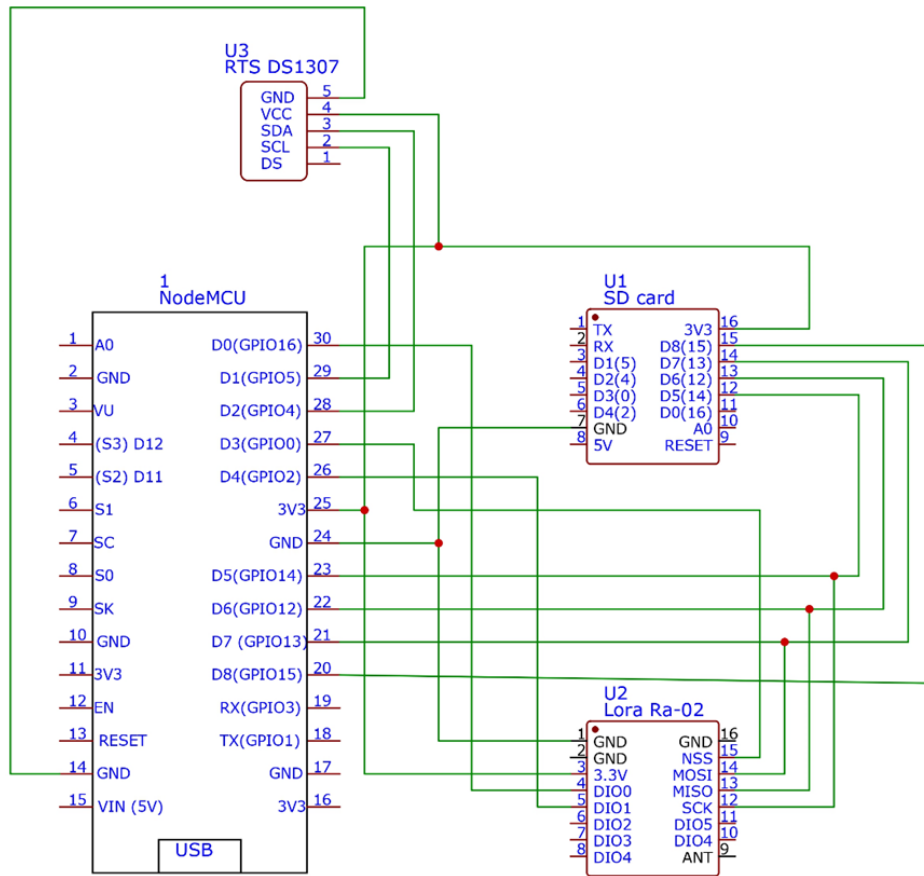
Table 6 below presents the material costs spent to assemble the DGS and WSD prototypes, excluding the labor costs.

Table 6

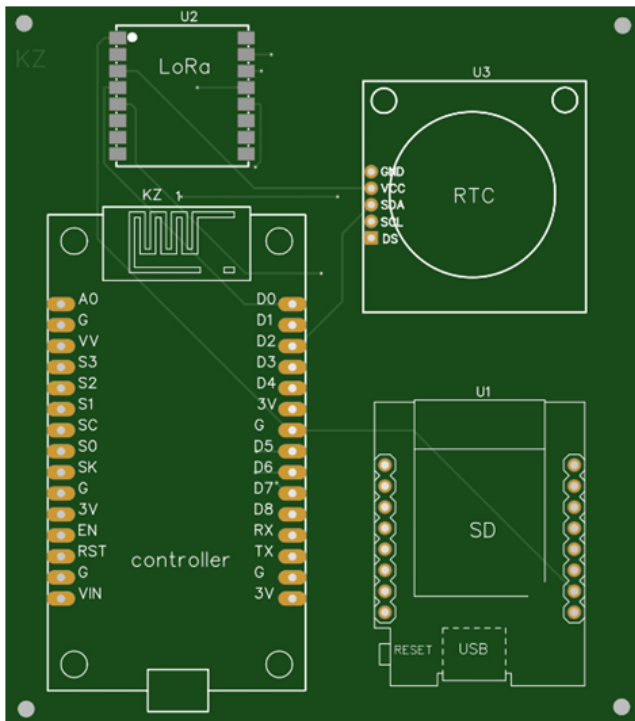
Material cost estimation

Units	Components	Price*, USD	Unit cost, USD
DGS	NodeMCU firmware (ESP-8266MOD and Wi-Fi)	6.74	90.54
	Lora Ra-02 on the SX1278 chip	7.63	
	RS-15-5 power supply	9.67	
	DS3231 RTC module	4	
	Schuko plug 230V	2	
	RobotDyn SD card module with microSD	4.5	
	Eagle software (monthly payment)	56	
WSD	ATmega328P microcontroller	6.2	79.53
	Lora Ra-02 on the SX1278 chip	7.63	
	RYD-F3-2 case	10	
	Two LS 14500 batteries	12	
	TOF400 VL53L1X sensor	18.15	
	TF-Luna Benewake sensor	24.9	
	YL-63 sensor	0.65	
Overall cost, USD			170.07

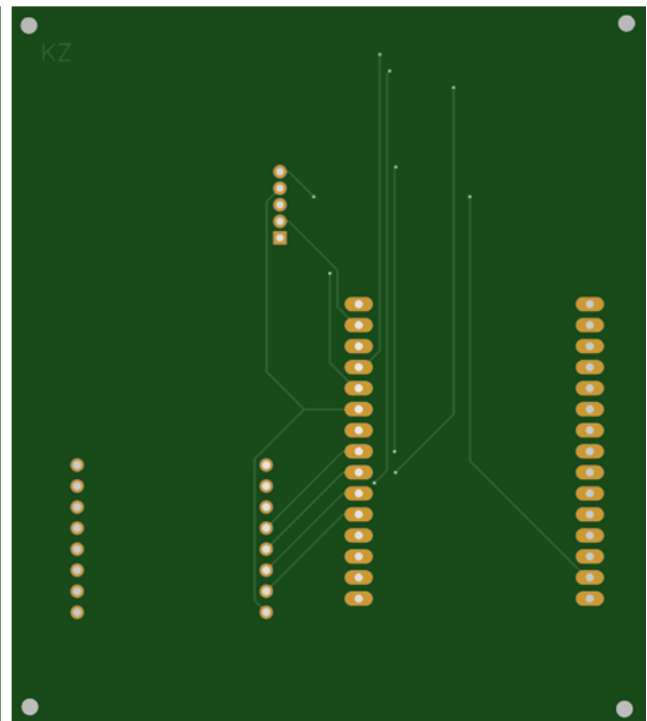
Note: * – since the components were purchased locally, the prices were converted according to the exchange rate for the date 31.03.2023 [36], which was 448.05 KZT for 1 USD



a

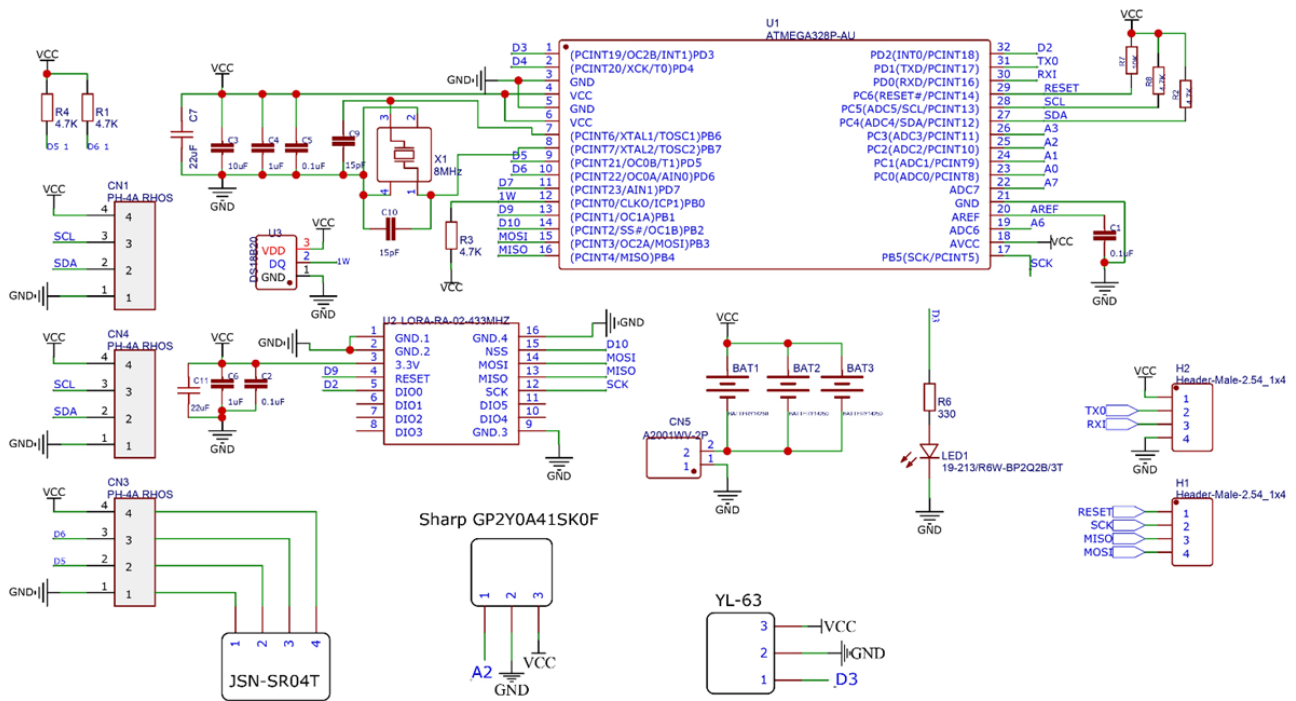


b

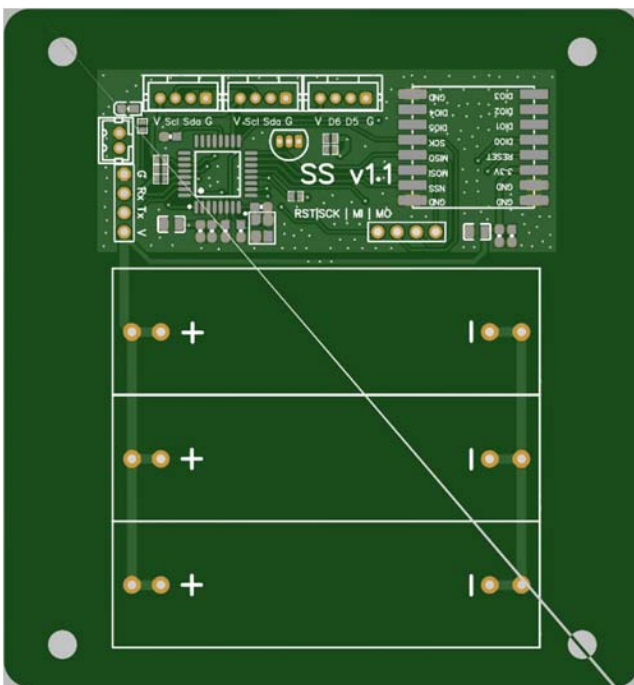


c

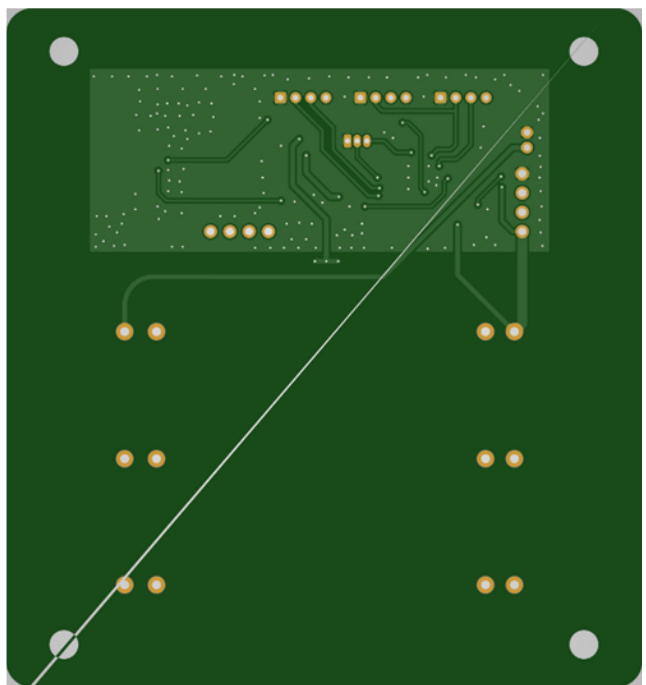
Fig. 3. Electronic scheme of DGS:
 a – circuit diagram; b – front side of 77×87 mm PCB; c – back side of 77×87 mm PCB



a



b



c

Fig. 4. Electronic scheme of WSD: a – circuit diagram; b – front side of 84×90 mm PCB; c – back side of 84×90 mm PCB

Table 6 shows that the total material cost for single units of DGS and WSD was approximately 170 USD, including around 90.54 USD for DGS and 79.53 USD for WSD. It is worth noting that the use of free software for PCB design instead of Eagle could save us 56 USD, and make the overall expenditure even less (around 114 USD).

The cost can be reduced even more through mass production. The equipment will need to be serviced. Therefore, it is possible to consider a service business model based on monthly equipment rental, which will allow obtaining the hardware and software complex without the need for large capital investments.

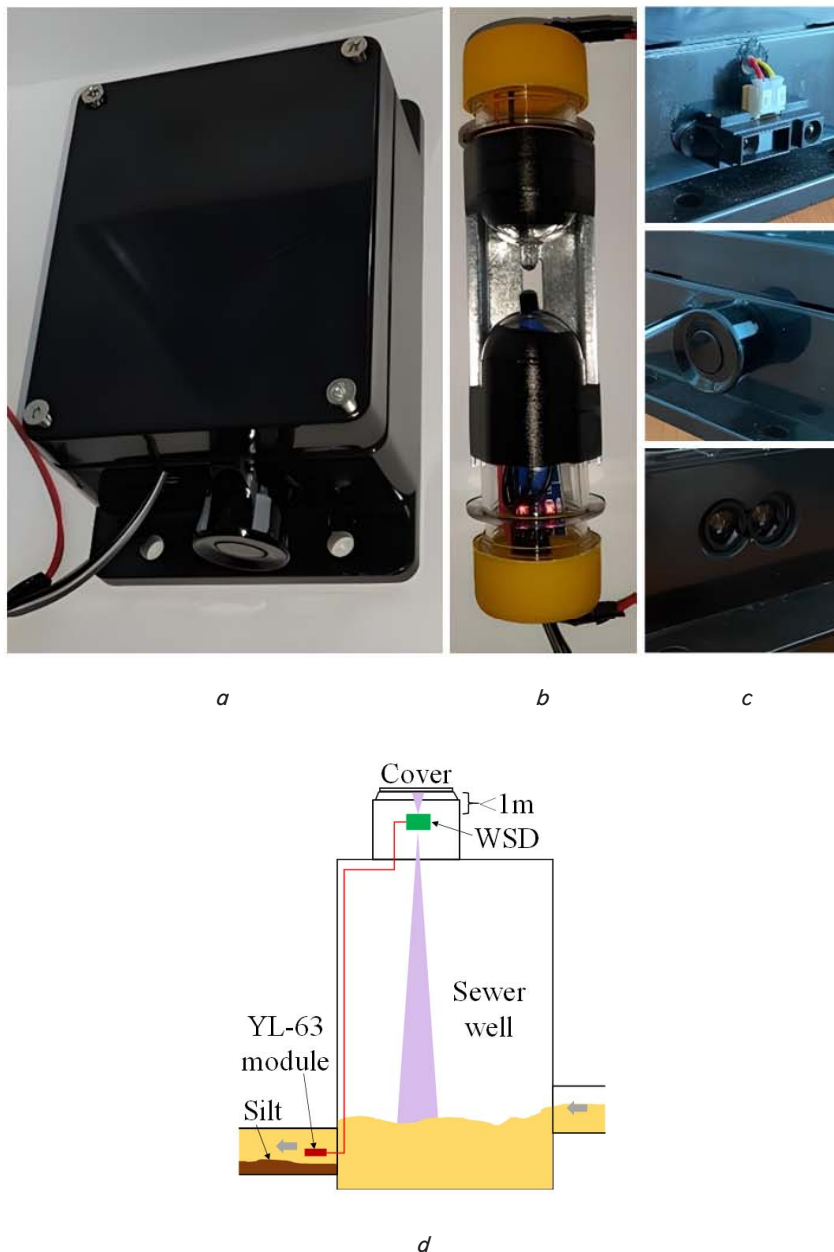


Fig. 5. Prototype of WSD and its installation schema:
a – main unit; *b* – external unit;
c – sensor options; *d* – operating diagram

5.3. Testing and evaluating the accuracy of various integrated sensors

Fig. 6 shows the results of sensor tests imitating a measurement of the distance to the manhole cover, ranging from 0.2 to 1.0 m.

The above graphs depict that the TOF400 VL53L1X laser sensor provides measurements closest to the intended distances (between 0.2 and 1.0 m) with a relatively small standard deviation within the range of 0.13 and 0.24. However, it should be noted that at short distances up to 0.4 m, the TF-Luna Benewake LiDAR sensor offered more stable measurements with the lowest frequency of oscillations. On the other hand, the Sharp GP2Y0A41SK0F infrared sensor provided the worst results. Its measurements at distances

between 0.4 and 1.0 m remained within the range of 0.13–0.23 m, indicating its unsuitability for monitoring manhole covers.

Fig. 7 displays the results of the sensor tests simulating a measurement of the wastewater level in a sewage well, ranging from 1.0 to 5.0 m.

From the graphs above, it is evident that the TF-Luna Benewake LiDAR sensor displayed the most favorable outcomes at distances ranging from 1.0 to 5.0 meters. The standard deviation for this sensor was within the range of 0.44 to 1.15. The TOF400 VL53L1X laser sensor ranked second in performance, but its standard deviation exhibited significant variation (up to 125.57). Additionally, its inaccuracy and oscillation frequency increased as the distance of the obstacle increased. The JSN-SR04T ultrasonic sensor delivered the poorest results within this distance range. Although the standard deviation (ranging from 0.0 to 26.05) was lower than that of the other sensors, the readings from this sensor remained fixed at 0.22–0.23 m when tested at distances between 2.0–5.0 m.

Fig. 8 shows the analysis of measurement deviations of the TF-Luna Benewake Li-DAR sensor and the TOF400 VL53L1X laser sensor.

The analysis of deviations in Fig. 8 showed that as the distance increased, the measurement accuracy of both sensors decreased. At distances up to 2.0 meters, the accuracy rates lie within ± 5 cm. At longer distances, there was a sharp decrease in the accuracy of the TOF400 VL53L1X laser sensor, while the accuracy of the TF-Luna Benewake LiDAR sensor remained no worse than ± 8 cm up to 5.0 m. Therefore, the TOF400 VL53L1X turned out to be more suitable for monitoring the manhole cover, while the TF-Luna Benewake appeared to be better for wastewater level monitoring. Fig. 8

also shows the equations that can be used to roughly estimate the accuracy level of the aforementioned sensors depending on the measured distance. For TF-Luna Benewake, the equation is expressed as a logarithmic function with a reliability level of $\approx 84.5\%$, while for TOF400 VL53L1X, it is expressed as an exponential function with a reliability level of $\approx 89.6\%$. Thus, for a measurement distance of 8–10 m, the accuracy of the TF-Luna Benewake sensor would not exceed an acceptable range of ± 10 cm. Based on the results of the sensor tests, it became necessary to replace the sensors in the initially assembled WSD combinations as follows: TF-Luna Benewake – for measuring wastewater level; TOF400 VL53L1X – for detecting the presence of manhole cover.

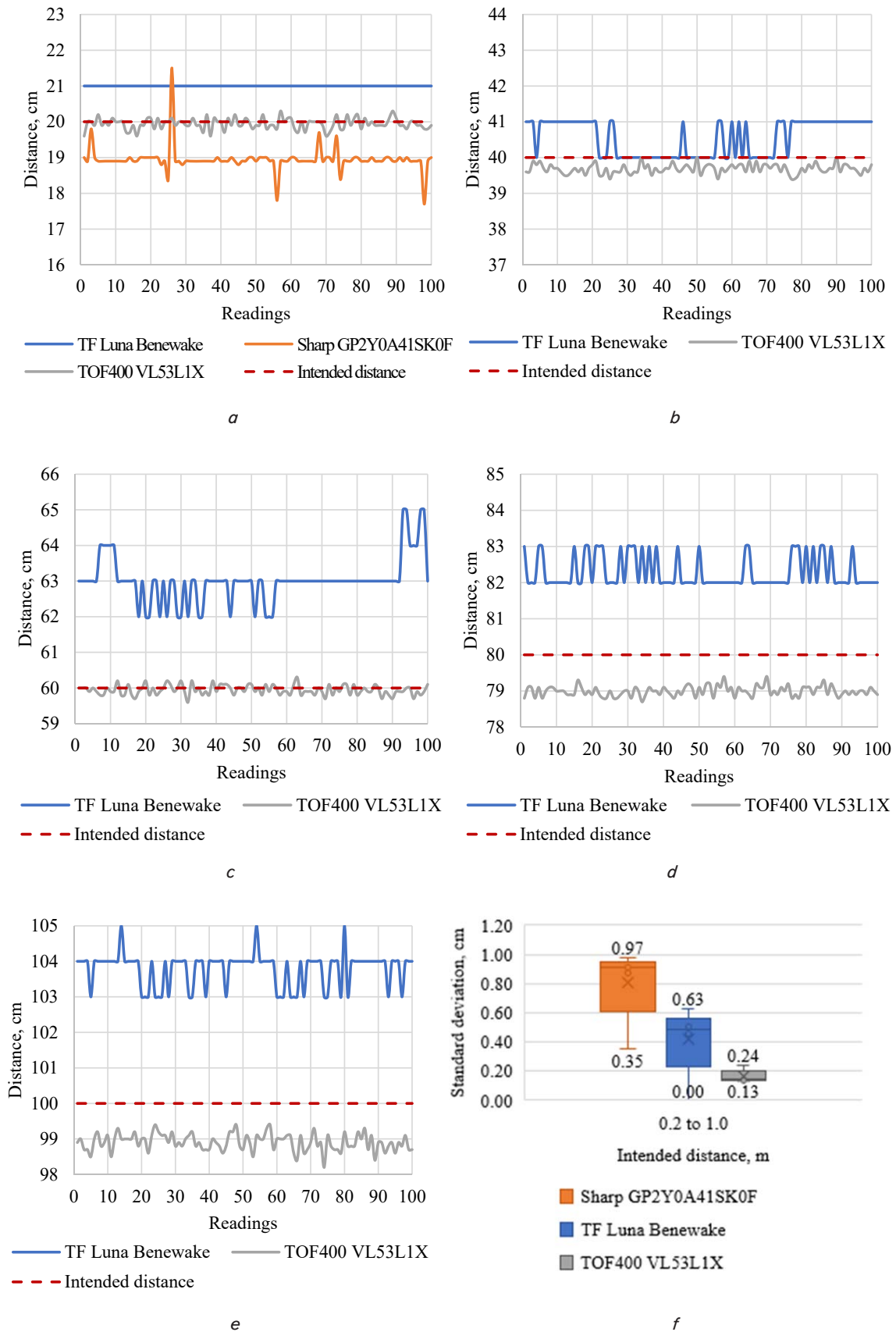


Fig. 6. Testing of sensors at intended distances from 0.2 to 1.0 m:
 a – 0.2 m; b – 0.4 m; c – 0.6 m;
 d – 0.8 m; e – 1.0 m; f – standard deviation

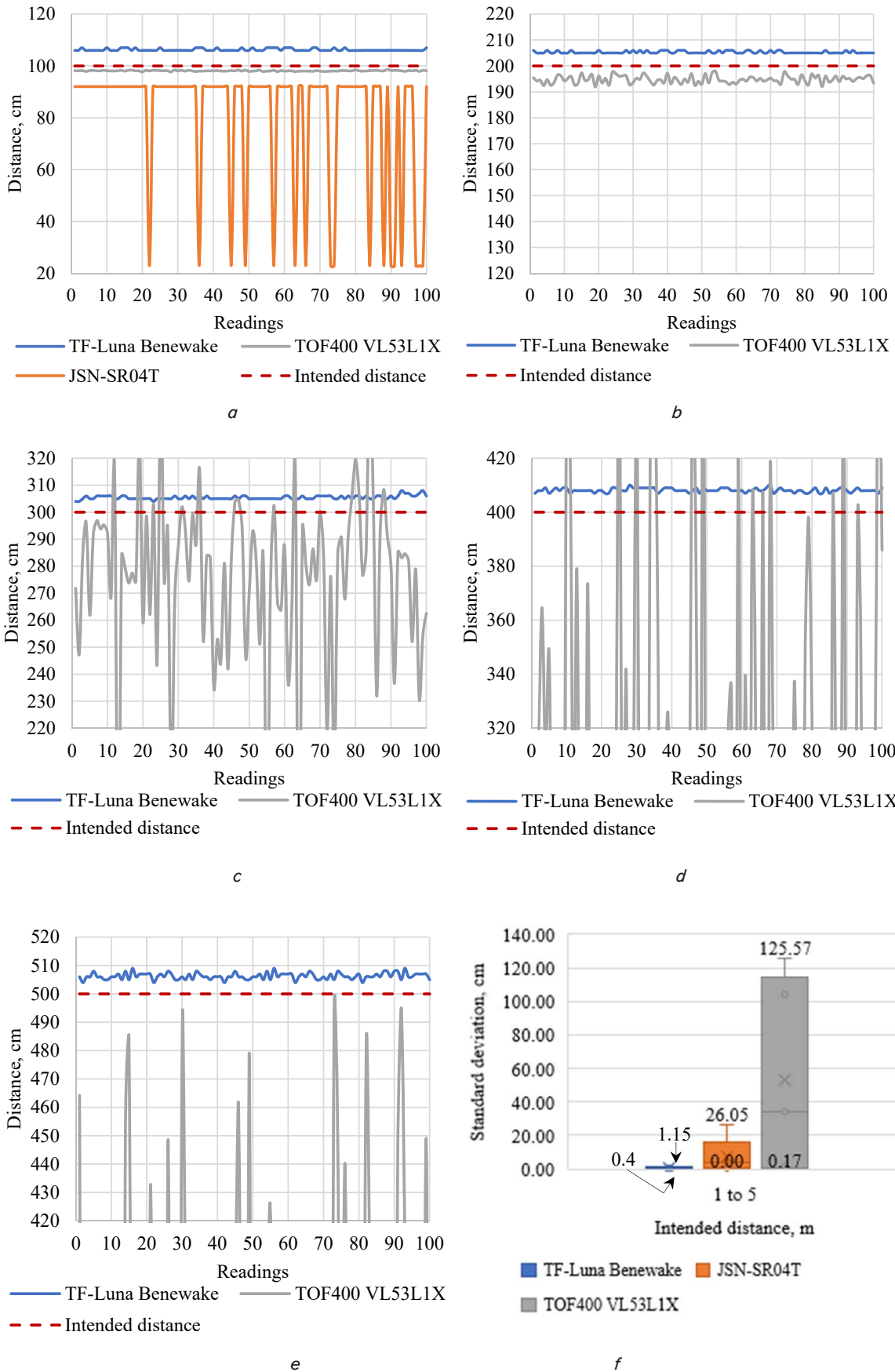


Fig. 7. Testing of sensors at intended distances from 1.0 to 5.0 m: *a* – 1.0 m; *b* – 2.0 m; *c* – 3.0 m; *d* – 4.0 m; *e* – 5.0 m; *f* – standard deviation

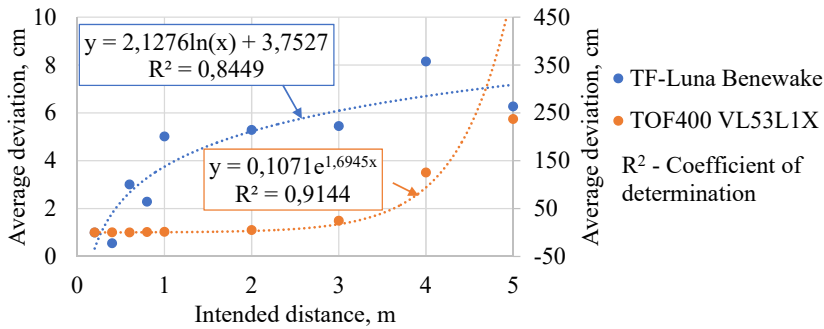


Fig. 8. Deviation analysis

5. 4. Algorithms to detect sewage system problems using integrated sensors

Fig. 9 below shows the proposed layout of the WSD installation and algorithms integrated to GIS.

According to the figure above, the WSD is anchored to the shaft section of the sewage well at a certain distance from the bottom of the manhole cover, while the external unit is fixed on the middle diameter of the outlet pipe on its inner wall (Fig. 9, a).

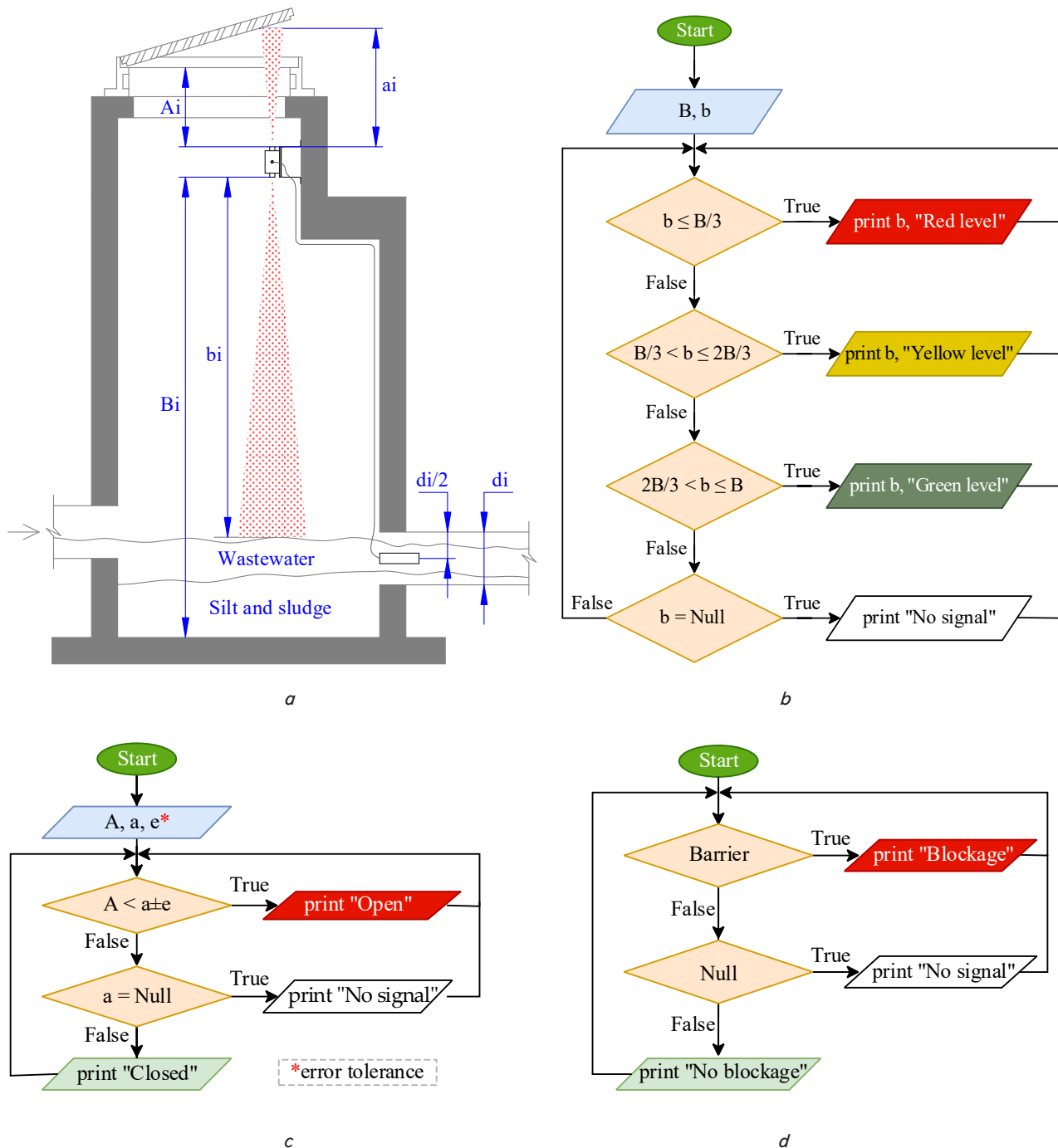


Fig. 9. Sewage monitoring algorithms integrated to GIS: a – sewage well section; b – wastewater overflow algorithm; c – manhole cover presence algorithm; d – pipe blockage algorithm

As mentioned above, the ATmega328P microcontroller used for WSD allows utilizing additional sensors. So, in cases of several outlet pipes in the sewage well, several external units can be connected to WSD. Additionally, the figure highlights the key parameters of the system, including A , a , B , b , d , and e , which represent the distance from the WSD upward-facing sensor (i.e. TOF400 VL53L1X) to the manhole cover bottom, the actual distance to any obstacle measured by the TOF400 VL53L1X, the constant distance from the WSD downward-facing sensor (TF-Luna Benewake) to the bottom of the sewage well, the actual distance to the wastewater level measured by the TF-Luna Benewake, the diameter of the outlet pipe, and the error tolerance that can be assigned by the end user of RTSMS. The figure also includes three algorithms for detecting sewer overflows, the presence/absence of manhole cover, and detecting pipe blockage. The overflow algorithm in Fig. 9, b utilizes parameters B and b to test four sequential conditions that are continuously executed in a loop, generating “Red”, “Yellow”, and “Green” alerts for different wastewater levels, and a “No signal” message if Null data retrieved. The algorithm in Fig. 9, c uses parameters A , a , and e to determine whether the manhole is open, closed, or “No signal” message if Null data retrieved. The last algorithm in Fig. 9, d tests for the presence of any barrier (silt or sludge) in the outlet pipe and alerts “Blockage” if true, and “No blockage” if false or “No signal” message if Null data retrieved. Overall, Fig. 8 provides a comprehensive illustration of the sewage well system and associated algorithms, allowing for effective monitoring and management of wastewater systems using GIS.

5. 5. Web-based Geographic Information System

Fig. 10 below illustrates the user interface of the developed GIS.

As illustrated in the above figure, the GIS interface enables real-time tracking of the condition of sewer manholes and pipes on an interactive map. The base map is generated using the OpenLayers library and includes three types: Open Street Map (OSM), satellite, and hybrid. At the software level, the direction of wastewater flow between manholes through pipes is determined, and algorithms presented in Fig. 9, $b-d$ are implemented.

The symbols used to represent manholes come in six variations. For example, a circle with a cross or a checkmark indicates an open or closed manhole, respectively, and colors such as red, yellow, or green indicate the wastewater level in the manholes. Pipes between manholes are colored green or red depending on whether they are blocked or not. Clicking on a manhole or pipe displays a message about its status. In the current version of the interface, there are no tools for drawing the manhole and pipe system. The location data and constant and variable parameters are manually assigned and linked to the WSD on the server side. In the future, it is planned to implement this missing feature, as well as add a tool for uploading external files in GeoJson and Shapefile formats containing spatial information about manholes and pipes. All the components for the GIS development are open-source and freely available.

6. Discussion of the results of the prototype development of an integrated IoT-based real-time sewer monitoring system using low-power sensors

The results obtained can be attributed to the thorough investigation and selection of suitable microelectronic components, software, and firmware development platforms for the real-time sewer monitoring system. The chosen system architecture (Fig. 2), based on the Internet of Things concept, enables wireless communication between the data gathering station (Fig. 3) and the sensing devices (Fig. 4, 5), facilitating continuous monitoring of sewer chambers, pipes, and manhole covers. The sensor testing results (Fig. 6–8) provide valuable insights into the performance of different sensors in measuring distance, allowing for informed decision-making in selecting appropriate sensors for specific monitoring tasks. The designed algorithms (Fig. 9) that utilize various fixed parameters and dynamic sensory data provide alert statuses for wastewater level, manhole cover presence, and outlet pipe blockage. The developed web-based GIS (Fig. 10) enables real-time visualization of the current status the algorithms (Fig. 9) provide in an interactive manner. The material costs (Table 6) spent for the prototyping amounted to roughly 170 USD.



Fig. 10. Interface of RTSMS GIS

The obtained results offer several notable features compared to existing approaches. Firstly, the use of low-power microelectronic components and wireless technologies ensures the durability and continuous operation of the monitoring devices. This is particularly important for sewer monitoring, where the devices need to withstand challenging environmental conditions. Secondly, the system architecture allows for real-time monitoring of an entire city's sewer system, providing a comprehensive view of the system's status, rather than only during inspections, as suggested in [7, 12]. Thirdly, the integration of GIS technology and web-based visualization enables the interactive and user-friendly representation of the monitoring data, facilitating efficient data analysis and decision-making. The solutions discussed in [7, 12] do not seem to offer a viable feature. Additionally, the overall cost of the solution is relatively low (around 170 USD) when compared to existing solutions proposed by [12, 54–59].

Despite the promising results, this study has certain limitations. Firstly, the evaluation of sensor performance is based on specific imitative conditions and may not fully capture all possible scenarios encountered in real-world sewer systems. The study primarily focuses on the performance of sensors in measuring distance, while other parameters, such as water flow rate or pressure, are not considered. Additionally, the study assumes a fixed set of parameters common to most sewer chambers, which may not accurately represent the diverse range of sewer systems found in different locations.

There are a few notable limitations in this study that could be addressed in future research. Firstly, expanding the range of sensor testing to include a wider variety of sensor types and models could provide more comprehensive insights into their performance characteristics. Additionally, conducting field trials in different sewer systems with varying conditions would help validate the effectiveness and reliability of the proposed monitoring system. Furthermore, incorporating additional parameters such as water flow rate and pressure into the algorithm design could enhance the system's capability to detect and predict sewer system anomalies. Lastly, conducting a cost-benefit analysis to evaluate the long-term economic viability of implementing the monitoring system on a larger scale would provide valuable information for decision-makers.

The future development of this research could involve further refinement and optimization of the algorithms used for detecting sewage overflow, manhole cover presence, and pipe blockage. Fine-tuning these algorithms based on more extensive data collection and analysis could enhance their accuracy and reliability. Additionally, the integration of advanced data analytics techniques, such as machine learning algorithms, could enable predictive maintenance and early warning systems for sewer infrastructure. However, the development of such predictive models may encounter challenges related to data availability, model complexity, and the need for robust mathematical models to handle the inherent uncertainties in sewer system dynamics. Further interdisciplinary collaboration between engineering, data science, and mathematics could help overcome these difficulties and advance the field of real-time sewer monitoring.

7. Conclusions

1. Investigation of various microelectronic components, software and firmware development platforms, databases

and APIs identified a suitable system architecture for the real-time sewer monitoring system based on the Internet of Things concept. According to the architecture, the wireless sensing devices are mounted inside the sewer chamber at a maximum depth of 1 m. The two integrated sensors of the device are pointed upwards on the manhole cover and downwards on the bottom of the chamber, and the external units are mounted in the outlet pipes. The data gathering station can simultaneously communicate with an unlimited number of sensing devices in the radius of up to 10 km via LoRaWAN protocol, and send the monitoring data to the server using Wi-Fi internet. The server side receives the data by HTTP requests and stores it in the database. The client side dynamically visualizes the data in JSON format on a browser using web-map API. Such an architecture can serve an entire city's sewer system, hence be adapted for other monitoring purposes as well.

2. The use of low-power microelectronic components and wireless technologies helps to build durable and affordable devices that enable continuous condition monitoring of sewer chambers, pipes and manhole covers. Thus, the results demonstrate the circuit design and assembly of the data gathering station (based on NodeMCU firmware) and wireless sensing device (based on ATmega328P chip). The data gathering station utilizes modules such as LoRa Ra-02, DS3231 RTC, and RobotDyn SD card, connected via a 77×87 mm PCB. The wireless sensing device, on the other hand, incorporates various sensor combinations, including the Sharp GP2Y0A41SK0F, TOF400 VL53L1X, JSN-SR04T, TF-Luna Benewake, and communicates with the data gathering station through the 433 MHz LoRa Ra-02 module. Its 84×90 mm PCB with connected micro components fit into an RYD-F3-2 case, with the YL-63 module externally assembled. The recommended installation involves fixing the device inside the sewer chamber and mounting the YL-63 module on the outlet pipe at a midpoint height. The research demonstrates that the real-time sewer monitoring system can be built with affordable expenditure. Thus, it costs around 170 USD for the necessary materials, including 79.53 USD for wireless sensing devices and 90.54 USD for the data gathering station. It is expected that the costs can be reduced by mass production.

3. The sensor testing results indicate that the TOF400 VL53L1X laser sensor is best suited for measuring the distance to the manhole cover, providing measurements closest to the intended distances with a relatively small standard deviation of 0.13–0.24 cm. However, the TF-Luna Benewake LiDAR sensor provides more stable measurements at shorter distances of up to 0.4 m with a standard deviation of 0.0–0.63 cm. The Sharp GP2Y0A41SK0F infrared sensor performed the worst in monitoring manhole covers, giving inappropriate measurements at distances greater than 0.2 m with a standard deviation of 0.35–0.97 cm. For wastewater level measurement, the TF-Luna Benewake LiDAR sensor demonstrated the best performance within the range of 1.0 to 5.0 m with a standard deviation of 0.44–1.15 cm. The TOF400 VL53L1X laser sensor ranked second, but its standard deviation showed significant variation as the distance increased (0.17–125.57 cm) due to frequent oscillation of measurements. In contrast, the JSN-SR04T ultrasonic sensor delivered the least satisfactory results due to the inability to measure beyond 2.0 m. Although its standard deviation within the distance range of 1.0 to 5.0 m was 0.0–26.05 cm (better than TOF400 VL53L1X). The analysis of deviations

revealed that both sensors experienced a decrease in measurement accuracy as the distance increased. The TOF400 VL53L1X sensor showed an accuracy of ± 1 cm up to 3 m distance being more suitable for monitoring manhole covers, while TF-Luna Benewake showed a more stable trend in greater distances being more suitable for wastewater level monitoring. The exponential and logarithmic functions expressing the accuracy trends of TOF400 VL53L1X and TF-Luna Benewake can be recommended for rough projection of their accuracy levels in various distances (even more than 5.0 m) with 89.6 % and 84.5 % confidence levels, respectively.

4. The system of parameters most common to the majority of sewer chambers in combination with sensory data may help in designing proper algorithms to detect sewage overflow, manhole cover presence and pipe blockage. Such parameters include fixed distances from sensors to the manhole cover (a) and the bottom of a sewer chamber (b), diameter of outlet pipe (d), user defined error tolerance (e), as well as dynamic distance measurements of sensors (a , b), as indicated in Fig. 9. Thus, the study demonstrates three algorithms that manipulate the digital (distance measurements from TOF400 VL53L1X and TF-Luna Benewake) and Boolean (barrier or barrier free outputs from YL-63) parameters along with chamber-specific fixed parameters and alert status information, which can be further used for visualization purposes. The first algorithm alerts red, yellow and green status depending on the wastewater level in a chamber. The second algorithm alerts the open or closed status of the manhole cover. The third algorithm alerts the blockage or no blockage status of outlet pipes.

5. The web-based GIS based on OpenLayers API turned out to be a suitable instrument to visually represent the real-time status of sewer manholes and pipes interactively. The GIS implemented in this research has three base layers (OSM, satellite and hybrid). Six types of point features were used to demonstrate the overflow and presence status

of manholes that are distinguished by color and symbol. The line features with changing color (green or red) and arrows were used to demonstrate pipe blockage status and the direction of wastewater flow. Any visual change in features stems from the current status that the integrated algorithms alert continuously. The software solutions for the implementation of GIS were free of charge. Further work on the GIS will focus on increasing the functionality.

Conflict of interest

The authors declare that they have no conflict of interest in relation to this research, whether financial, personal, authorship or otherwise, that could affect the research and its results presented in this paper.

Financing

This research was funded by the Science Committee of the Ministry of Science and Higher Education of the Republic of Kazakhstan (Grant № AP09057970).

Data availability

Data will be made available on reasonable request.

Acknowledgments

The authors acknowledge research group members Prof. Dr. Assel Tulebekova, Assoc. Prof. Dr. Zhanbolat Shakhmov, and Dr. Sungat Akhazhanov for their valuable contribution to implementing the current study under Grant № AP09057970.

References

- Jia, Y., Zheng, F., Maier, H. R., Ostfeld, A., Creaco, E., Savic, D. et al. (2021). Water quality modeling in sewer networks: Review and future research directions. *Water Research*, 202, 117419. doi: <https://doi.org/10.1016/j.watres.2021.117419>
- Kolesnikova, O., Vasilyeva, N., Kolesnikov, A., Zolkin, A. (2022). Optimization of raw mix using technogenic waste to produce cement clinker. *Mining Informational and Analytical Bulletin*, 10-1, 103–115. doi: https://doi.org/10.25018/0236_1493_2022_101_0_103
- Kolesnikova, O., Syrlybekkyzy, S., Fediuk, R., Yerzhanov, A., Nadirov, R., Utebayeva, A. et al. (2022). Thermodynamic Simulation of Environmental and Population Protection by Utilization of Technogenic Tailings of Enrichment. *Materials*, 15 (19), 6980. doi: <https://doi.org/10.3390/ma15196980>
- Patil, V., Kadam, A. (2022). Problems and Perspectives of the Urban Sewage System: A Geographical Review. *RESEARCH REVIEW International Journal of Multidisciplinary*, 4, 2815–2819. URL: https://www.researchgate.net/publication/360388311_Problems_and_Perspectives_of_the_Urban_Sewage_System_A_Geographical_Review
- Sojobi, A. O., Zayed, T. (2022). Impact of sewer overflow on public health: A comprehensive scientometric analysis and systematic review. *Environmental Research*, 203, 111609. doi: <https://doi.org/10.1016/j.envres.2021.111609>
- Mok, C. M. E., Wong, K., Shea, Y. K. G., Chen, W., Cheng, S. C. L. (2014). Design and algorithm development of an expert system for continuous health monitoring of sewer and storm water pipes. *International Conference on Underground Utility*.
- Patil, R., Ansari, S., Kaur Calay, R., Mustafa, M. (2021). Review of the State-of-the-art Sewer Monitoring and Maintenance Systems Pune Municipal Corporation - A Case Study. *TEM Journal*, 10 (4), 1500–1508. doi: <https://doi.org/10.18421/tem104-02>
- Czimmermann, T., Ciuti, G., Milazzo, M., Chiurazzi, M., Roccella, S., Oddo, C. M., Dario, P. (2020). Visual-Based Defect Detection and Classification Approaches for Industrial Applications—A SURVEY. *Sensors*, 20 (5), 1459. doi: <https://doi.org/10.3390/s20051459>
- Beheshti, M., Sægrov, S. (2019). Detection of extraneous water ingress into the sewer system using tandem methods – a case study in Trondheim city. *Water Science and Technology*, 79 (2), 231–239. doi: <https://doi.org/10.2166/wst.2019.057>

10. Tuomari, D. C., Thompson, S. (2004). "Sherlocks of stormwater" effective investigation techniques for illicit connection and discharge detection. *Proceedings of the Water Environment Federation*, 2004 (16), 1252–1259. doi: <https://doi.org/10.2175/193864704784147098>
11. Martini, A., Troncosi, M., Rivola, A. (2016). Leak Detection in Water-Filled Small-Diameter Polyethylene Pipes by Means of Acoustic Emission Measurements. *Applied Sciences*, 7 (1), 2. doi: <https://doi.org/10.3390/app7010002>
12. Moradi, S., Zayed, T. (2017). Real-Time Defect Detection in Sewer Closed Circuit Television Inspection Videos. *Pipelines 2017*. doi: <https://doi.org/10.1061/9780784480885.027>
13. Wai-Lok Lai, W., Dérobert, X., Annan, P. (2018). A review of Ground Penetrating Radar application in civil engineering: A 30-year journey from Locating and Testing to Imaging and Diagnosis. *NDT & E International*, 96, 58–78. doi: <https://doi.org/10.1016/j.ndteint.2017.04.002>
14. James, C. S. (2019). Flow-Measuring Structures. *Hydraulic Structures*, 243–282. doi: https://doi.org/10.1007/978-3-030-34086-5_7
15. Wang, Y., Li, P., Li, J. (2022). The monitoring approaches and non-destructive testing technologies for sewer pipelines. *Water Science and Technology*, 85 (10), 3107–3121. doi: <https://doi.org/10.2166/wst.2022.120>
16. Frehmann, T., Niemann, A., Ustohal, P., Geiger, W. F. (2002). Effects of real time control of sewer systems on treatment plant performance and receiving water quality. *Water Science and Technology*, 45 (3), 229–237. doi: <https://doi.org/10.2166/wst.2002.0083>
17. Rony, J. H., Karim, N., Rouf, MD. A., Islam, Md. M., Uddin, J., Begum, M. (2021). A Cost-Effective IoT Model for a Smart Sewerage Management System Using Sensors. *J*, 4 (3), 356–366. doi: <https://doi.org/10.3390/j4030027>
18. Alshami, A., Elsayed, M., Mohandes, S. R., Kineber, A. F., Zayed, T., Alyanbaawi, A., Hamed, M. M. (2022). Performance Assessment of Sewer Networks under Different Blockage Situations Using Internet-of-Things-Based Technologies. *Sustainability*, 14 (21), 14036. doi: <https://doi.org/10.3390/su142114036>
19. Utepov, Y., Kazkeyev, A., Aniskin, A. (2021). A multi-criteria analysis of sewer monitoring methods for locating pipe blockages and manhole overflows. *Technobius*, 1 (4), 0006. doi: <https://doi.org/10.54355/tbus/1.4.2021.0006>
20. Duran, O., Althoefer, K., Seneviratne, L. D. (2002). State of the art in sensor technologies for sewer inspection. *IEEE Sensors Journal*, 2 (2), 73–81. doi: <https://doi.org/10.1109/jsen.2002.1000245>
21. Pendharkar, A., Chillapalli, J., Dhakate, K., Gogoi, S., Jadhav, Y. (2020). IoT Based Sewage Monitoring System. *SSRN Electronic Journal*. doi: <https://doi.org/10.2139/ssrn.3697395>
22. Chillapalli, J., H. Jadhav, Y. (2020). IoT based Sewage gas Monitoring and Alert System using Raspberry PI. *International Journal of Scientific Research in Computer Science, Engineering and Information Technology*, 6 (4), 567–573. doi: <https://doi.org/10.32628/cseit12064114>
23. Amutha, M., Kamali, S., Sherli, T. (2022). Smart Manhole Managing and Monitoring System using IoT. *Proceedings of The International Conference on Emerging Trends in Artificial Intelligence and Smart Systems, THEETAS 2022*. Jabalpur. doi: <https://doi.org/10.4108/eai.16-4-2022.2318149>
24. Ilamurugan, G., Akiladevi, R. (2017). Integrated detection of open drainage and overflow, current leakage and rbage monitoring in IoT environment. *International Journal of Creative Research Thoughts*, 5 (4), 2602–2607. URL: <https://ijcrt.org/papers/IJCRT1704337.pdf>
25. Jan, F., Min-Allah, N., Saeed, S., Iqbal, S. Z., Ahmed, R. (2022). IoT-Based Solutions to Monitor Water Level, Leakage, and Motor Control for Smart Water Tanks. *Water*, 14 (3), 309. doi: <https://doi.org/10.3390/w14030309>
26. Yu, Y., Safari, A., Niu, X., Drinkwater, B., Horoshenkov, K. V. (2021). Acoustic and ultrasonic techniques for defect detection and condition monitoring in water and sewerage pipes: A review. *Applied Acoustics*, 183, 108282. doi: <https://doi.org/10.1016/j.apacoust.2021.108282>
27. Bhosale, P., Mithapelli, S., Bollabattin, S., Patel, R., Bhalerao, A., Patil, D. D. (2021). IoT based system for detection of sewage blockages. *Information Technology in Industry*, 9 (1), 961–970. doi: <https://doi.org/10.17762/itii.v9i1.224>
28. Patel, N. (2014). A Sensor Based Web GIS System for Urban Sewage Monitoring. *International Journal of Engineering Research & Technology (IJERT)*, 3 (1), 1933–1936. URL: <https://www.ijert.org/research/a-sensor-based-web-gis-system-for-urban-sewage-monitoring-IJERTV3IS10805.pdf>
29. Häring, I. (2021). Models for Hardware and Software Development Processes. *Technical Safety, Reliability and Resilience*, 179–192. doi: https://doi.org/10.1007/978-981-33-4272-9_10
30. Ogura, H. (2005). Analog Output Type Distance Measuring Sensor GP2Y0A41SK0F. URL: https://www.sharpsde.com/fileadmin/products/Optoelectronics/Sensors/Specs/GP2Y0A41SK0F_25Apr05_Spec_ED05G101.pdf
31. TOF laser ranging sensor module. URL: <https://download.kamami.pl/p587523-H21c81639dd5346518ca0cabd3a832b4a1.jpg>
32. JSN SR04T DC 5V Ultrasonic Module Distance Measuring Transducer Sensor IO Port Waterproof For Arduino. URL: https://www.diy-more.cc/collections/sensor-module/products/high-accuracy-jsn-sr04t-dc-5v-ultrasonic-module-distance-measuring-transducer-sensor-io-port-waterproof-for-arduino?_pos=2&_sid=2c5c55d16&_ss=r
33. TF-Luna 8m Low Cost Distance Sensor Modul. URL: https://en.benewake.com/TF-Luna/index_proid_328.html
34. FC-28 Soil Hygrometer (Moisture) Sensor. URL: <https://www.uruktech.com/product/fc-28-soil-hygrometer-sensor/>
35. YL-63 Infrared & Photoelectric Sensor Modules. URL: <http://us.100y.com.tw/viewproduct.asp?MNo=95649>

36. Daily Official (market) Foreign Exchange Rates. URL: <https://nationalbank.kz/en/exchangerates/ezhednevnye-oficialnye-rynochnye-kursy-valyut>
37. ATmega328P. 8-Bit AVR Microcontroller with 32K Bytes In-System Programmable Flash. URL: https://ww1.microchip.com/downloads/en/DeviceDoc/Atmel-7810-Automotive-Microcontrollers-ATmega328P_Datasheet.pdf
38. ESP8266EX Datasheet. URL: https://www.espressif.com/sites/default/files/documentation/0a-esp8266ex_datasheet_en.pdf
39. NodeMCU ESP8266 Detailed Review. URL: <https://www.make-it.ca/nodemcu-details-specifications/#:-:text=UART>
40. SD Card Module (3.3V/5.0V Arduino-Compatible, Micro SD Reader/Writer). URL: <https://makersportal.com/shop/arduino-compatible-micro-sd-card-module>
41. Ra-02 LoRa Product Specification V1.1. URL: https://docs.ai-thinker.com/_media/lora/docs/c048ps01a1_ra-02_product_specification_v1.1.pdf
42. GSM/GPRS Module. SIM800L. URL: <https://simcom.ee/documents/SIM800L/SIM800L%20SPEC170914.pdf>
43. ABS Black Plastic Electronics Project Box Enclosure Hobby Case with Screws. URL: <https://digitalzakka.com/product/abs-black-plastic-electronics-project-box-enclosure-hobby-case-with-screws/>
44. Uteпов, Ye. B. (2021). Effect of the shape and structure of maturity sensor's plastic housing on its physico-mechanical properties. *Eurasian Physical Technical Journal*, 18 (3 (37)), 83–87. doi: <https://doi.org/10.31489/2021no3/83-87>
45. LS 14500. Primary Li-SOC12 cell. URL: https://www.saft.com/download_file/6X7JMGAnv3Fm6HdmtEv%252B2gtlbZ1bRRVHkjS11M6md92GD2EF7vU%252F3Oybbz3WOIG%252BxR8srpA5iCdJ%252FV3IQzTVHQyiTucngZKEg9KkYCLkowAvgG1huqyXUIQvO1qUkZjGCfaa8Bj8zATp1fXJjXWOMWYOmKIKGl%252B2HKVzqrqCKI1yMfBQ%253D%253D/Data.Sheet.pdf
46. 15W Single Output Switching Power Supply. URL: <https://www.meanwell-web.com/content/files/pdfs/productPdfs/MW/RS-15/RS-15-spec.pdf>
47. PCB design made easy for every engineer. URL: <https://www.autodesk.com/products/eagle/overview?term=1-YEAR&tab=subscription>
48. Arduino IDE 2.1.0. URL: <https://www.arduino.cc/en/software>
49. MariaDB Server: The open source relational database. URL: <https://mariadb.org/>
50. Why Spring? URL: <https://spring.io/why-spring>
51. The library for web and native user interfaces. URL: <https://react.dev/>
52. A high-performance, feature-packed library for all your mapping needs. URL: <https://openlayers.org/>
53. Extremely Accurate I2C-Integrated RTC/TCXO/Crystal. URL: <https://www.analog.com/media/en/technical-documentation/data-sheets/ds3231.pdf>
54. Gruber, G., Winkler, S., Pressl, A. (2005). Continuous monitoring in sewer networks an approach for quantification of pollution loads from CSOs into surface water bodies. *Water Science and Technology*, 52 (12), 215–223. doi: <https://doi.org/10.2166/wst.2005.0466>
55. Siemers, L., Dodd, J., Day, D., Kerr, D., LaGorga, J., Romano, P. (2011). Low Cost Overflow Monitoring Techniques and Hydraulic Modeling of A Complex Sewer Network. *Proceedings of the Water Environment Federation*, 2011 (5), 571–583. doi: <https://doi.org/10.2175/193864711802837363>
56. Wani, O., Scheidegger, A., Carbajal, J. P., Rieckermann, J., Blumensaat, F. (2017). Parameter estimation of hydrologic models using a likelihood function for censored and binary observations. *Water Research*, 121, 290–301. doi: <https://doi.org/10.1016/j.watres.2017.05.038>
57. Rasmussen, M. R., Thorndahl, S., Schaarup-Jensen, K. (2008). A Low Cost Calibration Method for Urban Drainage Models. 11th International Conference on Urban Drainage: Edinburgh International Conference Centre. URL: https://vbn.aau.dk/ws/portalfiles/portal/14970929/A_Low_Cost_Calibration_Method_for_Urban_Drainage_Models
58. Jeanbourquin, D., Sage, D., Nguyen, L., Schaeli, B., Kayal, S., Barry, D. A., Rossi, L. (2011). Flow measurements in sewers based on image analysis: automatic flow velocity algorithm. *Water Science and Technology*, 64 (5), 1108–1114. doi: <https://doi.org/10.2166/wst.2011.176>
59. Lo, S.-W., Wu, J.-H., Lin, F.-P., Hsu, C.-H. (2015). Visual Sensing for Urban Flood Monitoring. *Sensors*, 15 (8), 20006–20029. doi: <https://doi.org/10.3390/s150820006>